Published in final edited form as:

Curr Biol. 2020 February 24; 30(4): 600–609.e2. doi:10.1016/j.cub.2019.12.017.

Antagonistic inhibitory circuits integrate visual and gravitactic behaviors

Michaela Bostwick[*,1], **Eleanor L. Smith**[*,2], **Cezar Borba**[3], **Erin Newman-Smith**[3,4], **Iraa Guleria**[3], **Matthew J. Kourakis**[4], **William C. Smith**[3,4,5]

[1]Department of Psychological and Brain Sciences, University of California, Santa Barbara, CA, USA 93106

[2]Department of Neurobiology, Physiology, and Behavior, University of California, Davis, CA 95616

[3]Department of Molecular, Cell and Developmental Biology, University of California, Santa Barbara, CA, USA 93106

[4]Neuroscience Research Institute, University of California, Santa Barbara, CA, USA 93106

[5]Corresponding author and lead contact: w_smith@ucsb.edu

SUMMARY

Larvae of the tunicate *Ciona intestinalis* possess a central nervous system of 177 neurons. This simplicity has facilitated the generation of a complete synaptic connectome. As chordates and the closest relatives of vertebrates, tunicates promise insight into the organization and evolution of vertebrate nervous systems. *Ciona* larvae have several sensory systems, including the ocellus and otolith, which are sensitive to light and gravity, respectively. Here we describe circuitry by which these two are integrated into a complex behavior: the rapid reorientation of the body followed by upward swimming in response to dimming. Significantly, the gravity response causes an orienting behavior consisting of curved swims in downward-facing larvae, but only when triggered by dimming. In contrast, the majority of larvae facing upward do not respond to dimming with orientation swims – but instead swim directly upward. Under constant light conditions, the gravity circuit appears to be inoperable, and both upward and downward swims were observed. Using connectomic and neurotransmitter data we propose a circuit model that can account for these behaviors. The otolith consists of a statocyst cell and projecting excitatory sensory neurons (antenna cells). Postsynaptic to the antenna cells are a group of inhibitory primary interneurons, the antenna relay neurons (antRNs), which then project asymmetrically to the right and left motor units, thereby mediating curved orientation swims. Also projecting to the antRNs are inhibitory photoreceptor relay interneurons. These interneurons appear to antagonize the otolith circuit until they themselves are inhibited by photoreceptors in response to dimming, thus providing a triggering circuit.

[*]these two authors contributed equally to this work

AUTHOR CONTRIBUTIONS.

M.B., E.L.S. and I.G. performed experiments. C.B., E.N-S. and M.K. conceived and performed experiments. W.C.S. conceived and performed experiments, wrote the manuscript, and secured funding.

DECLARATION OF INTERESTS. The authors declare no competing interests.

Keywords

gravitaxis; *Ciona*; connectome; neural circuit

INTRODUCTION

Mechanisms to detect and respond to Earth's gravitational field are found widely throughout the kingdoms of life, both in unicellular and multicellular organisms [1–3]. In most animals, detection of gravity involves an organ with a dense mineralized mass and accompanying sensory cells. Vertebrate gravitactic organs are characterized by calcified otoliths of the vestibular system of the inner ear [4,5], while many invertebrates have mineralized statoliths that serve a similar function [6–8]. Gravity sensing organs modulate a range of animal behaviors, including taxis (termed gravitaxis), posture orientation, body movements, and gaze stabilization [9–11]. Both positive and negative gravitaxis is widely observed in animals, including in aquatic zooplankton [12–15], amphibian and teleost larvae [16,17], and in terrestrial invertebrates such as *Drosophila* and *Caenorhabditis japonica* [18,19]. Despite the widespread occurrence of gravitaxis, the neural circuitry underlying these behaviors is largely unknown. At present, the only comprehensive synaptic connectivity maps (*i.e.*, connectomes) are from two invertebrates: the adult nematode *Caenorhabditis elegans* [20] and a larva of the tunicate *Ciona intestinalis* [21]. While there are conflicting reports on whether *C. elegans* has a gravity response [18,22], *Ciona* larvae clearly do. The most commonly described gravitactic behavior in *Ciona* larvae is negative gravitaxis [23–25]. Although older reports have described an initial period of positive gravitaxis in newly hatched *Ciona* larvae [26], this may simply be the passive sinking of larvae, which are denser than water [27,28].

Ciona occupies a unique evolutionary position as an invertebrate chordate, and along with the other tunicate species comprise the closest extant relatives of the vertebrates [29]. The evolutionary kinship of tunicates and vertebrates is most evident in tunicate larvae, which have a highly conserved body plan shared with vertebrates that is marked by a notochord running the length of the tail, muscle cells on the right and left sides of the tail, and a dorsal and hollow central nervous system (CNS). The larval *Ciona* CNS has been the subject of particular interest and speculation. Despite having only 177 neurons, it has extensive anatomical and gene-expression homology to vertebrate CNSs, and develops from a simple neural plate following a well-described cell lineage [reviewed in [30]]. Gravitaxis in *Ciona* is mediated by a sensory apparatus that consists of a large otolith cell located in the ventricle of the brain vesicle (BV), two otolith-associated ciliated cells, and two glutamatergic antennae sensory neurons [Figure 1A and [21,31,32]]. Figure 1B shows a simplified minimal gravitaxis circuit in which like neurons and their connections (including strength) are combined, while Figure S1 shows the full circuit. The function of the otolith cell is evident from micrographs in which it can be seen tethered to the floor of the ventricle by a narrow stalk, but should otherwise be free to move as the larva changes position relative to gravity [33,34]. Interestingly, the *Ciona* otolith cell is not calcified like vertebrate otoliths, but rather appears to increase its density via the chelation of metal ions by large melanin-containing pigment granules, and loss of melanization of the otolith cell leads to a loss of gravitaxis

behavior [23,34]. In addition to not being calcified, the *Ciona* otolith cell has a very different ontogeny than the vertebrate otolith, originating from the central nervous system, rather than the otic placodes, as in vertebrates [35,36].

The function of the two otolith-associated ciliated cells is not known, but they are likely involved in detecting and transducing movements of the otolith cell. The two glutamatergic antenna cells are the sole sensory afferents of the gravity sensing apparatus and project their axons to a cluster of eleven interneurons in the posterior BV named *antenna relay neurons* (antRN) [Figures 1 and S1, and [21]]. The antRNs express *vesicular GABA transporter* (VGAT), and are likely GABAergic and inhibitory [37]. The antRNs send their projections through the narrow neck region of the CNS (thought to be homologous to the vertebrate midbrain/hindbrain boundary) to the motor ganglion (MG), which is thought to be homologous to the vertebrate hindbrain [CNS homologies reviewed in [30]]. The antRNs thus provide the only links between the antenna cells in the BV to the MG. The primary postsynaptic targets of the antRNs are the three right and three left cholinergic motor ganglion interneurons (MGIN R and MGIN L, Figure 1 and S1), which in turn synapse to the right and left motor neurons, also cholinergic (MN in Figure 1 and S1). In addition, a subset of antRNs also directly synapse on the MNs.

In this manuscript we present an expanded and quantified assessment of gravitaxis behavior in *Ciona* larvae. We find that the gravitaxis circuit has an exclusively inhibitory input on swimming behavior. Moreover, the gravitaxis and visual behaviors are tightly interconnected. We present a model of gravitaxis circuitry that draws on behavioral, connectomic and neurotransmitter use data, and that has as its central element left/right asymmetric inhibition of muscles that drive downward facing larvae into tumbling swims, but that is absent when larvae face upward.

RESULTS

Photoresponse and gravitaxis in *Ciona* larvae.

Because *Ciona* larvae are denser than water and will settle to the bottom of the dish used to observe them, we developed the behavioral set-up shown in Figure 2A. In this set-up, a vertically-mounted 6-cm petri dish containing larvae is held in position for 5 minutes to allow the larvae to adapt and settle to the bottom. The petri dish is then rotated slowly 180 degrees, and the behavior of the larvae is then captured while they are in suspension and drifting slowly downward. This set-up should more realistically reflect their behavior in the wild, where they are thought to cycle between drifting down and swimming up [15]. Importantly, this set-up allows the larvae to swim in all directions, rather than only upward or sideways from the bottom, as in some previous studies [24,34]. In our assay we recorded both spontaneous swims, and swims in response to changing visible light (505 nm) intensities, while recording with far-red light (700 nm). Two larval stages were examined, 21 hours post fertilization (hpf), which is approximately two hours after hatching, and 25-hpf. These larval stages were chosen based on our findings, and those of others, that larval behavior changed over these times scales [24,38].

Video 1 shows typical assays in which larvae at 21- and 25-hpf were initially illuminated with 505 nm light at 600 lux. The visible light was then turned off (referred to here as the *lights-off* condition), which triggered the rapid upward swimming of nearly all larvae (Video 1; Figures 2B). The *lights-off*-induced upward swimming was most pronounced at 25-hpf, but was also present in 21-hpf larvae (Figures 2B and C). To quantify larval behavior, we assessed the net swim direction of spontaneous swims in the 5-second interval immediately before *lights-off* , as well as induced swims in the 5 second interval following *lights-off*, and classified the swims as either being UP, sideways (SIDE), or DOWN, as indicated by the 45° segments in Figure 2C. Five seconds was chosen because this interval allowed sufficient distance to be covered by the larvae so the direction could be assessed, but without the larvae swimming out of frame or hitting the side of the petri dish (Figure 2B). Spontaneous swims were relatively rare before *lights-off*. We observed spontaneous swims in 28.2% ± 9.5% of 21-hpf larvae, and 22.1% ± 12.4% of 25-hpf larvae (averages are from three movies at each time interval; and 23–32 larvae were assessed in each video). By contrast, nearly all larvae swam in response to *lights-off* (93.1% ± 12% at 21-hpf; and 97.6% ± 2.1% at 25-hpf; averages of three videos; 32–57 larvae were assessed in each video). Similar behavior was observed in response to the dimming of light (rather than *lights-off*), but with fewer larvae responding and the swims being shorter. The behavioral responses of 25-hpf larvae to 6- and 10-fold light dimming are shown in Video 2 (19% ± 9.7% and 56.7% ± 6.3% of larvae responded to *lights-off* with 6- and 10-fold dimming, respectively). Dimming-induced swim times were found to be 6.4 ± 4.1 and 6.8 ± 2.8 seconds at 6-and 10-fold dimming, respectively (n=8 and 10, respectively). Swim times induced by *lights-off* could not be quantified because the larvae swam until they reached the edge of the petri dish, but were > 20 seconds.

The spatial distribution of swims is presented in Figure 2C, with the various conditions (*e.g.*, spontaneous and *lights-off* induced swims, and developmental age) numbered 1–6 in blue boxes. The swim data were compiled from three batches of larvae and three videos from each batch, with 20 swimming larvae scored for each video. The data are presented as percentages for each directional segment. In the interval before *lights-off*, larvae were observed to spontaneously swim upward, sideways, and downward, with only a slight upward bias at 25-hpf, which differed from 21-hpf larvae (condition 1 versus 5; Figure 2C and D). In contrast to spontaneous swims, nearly all 25-hpf larvae swam upward (98%) in response to *lights-off*. We investigated if the position of the visible light at the instant of lights-off provided a directional cue by positioning it either above (Top Illumination) or below (Bottom Illumination) the petri dish. No difference was observed (condition 2 versus 4; Figure 2D), indicating that the only directional cue is gravity. At 21-hpf, the swim trajectories induced by *lights-off* were more varied, but with the majority (58%) of larvae swimming upward, and significantly different than the distribution of spontaneous swims at this stage (conditions 5 and 6; Figure 2D). We also quantified the spatial distribution of swims for 25-hpf larvae subjected to 6- and 10-fold dimming, rather than *lights-off* (Figure 2E). Because only a fraction of larvae responded to dimming, we only scored larvae that swam for >10 frames (~1 second). For both dimming stimuli we observed biased upward swimming, although with a lower percentage of larvae than with *lights-off* (Figure 2E). Finally, the *lights-off* induced swims of 21 hpf larvae were qualitatively different than those

of 25-hpf larvae, with the 25-hpf the *lights-off* induced swims being faster (25-hpf = 4.56 ± 0.69 mm/s vesus 21-hpf = 2.97 ± 0.36 mm/s; n= 28 for both time points; $p = 2.91 \times 10^{-15}$), and straighter, as quantified by measuring swim tortuosities (Figure 2F; $p = 2.02 \times 10^{-4}$), as described previously [38].

At the instant of *lights-off* we observed that most larvae were stationary and downward facing (Video 1). Consequently, upward *lights-off* induced swims required that these larvae reorient by first following a curved or tumbling swim trajectory until they faced upward, and then proceed in a straight path (Video 3, Figure 3A). This reorientation behavior was observed in 100% of downward facing larvae assessed at 25-hpf (average from three movies; n=60 larvae assayed). In addition to the downward-facing larvae, we were also able to find a small number of stationary 25-hpf larvae that were facing up or sideways at the instant of *lights-off*. The behavior of the sideways facing larvae was very similar to the downward facing larvae, with 95.7% ± 7.5 (n=33) initiating curved reorientation swims in response to lights-off. By contrast, the majority of upward facing larvae (53.8%; n=17) swam directly upward at lights-off with no obvious reorientation behavior (Video 3; Figure 3A), while the remainder showed short tumbling swims before proceeding to swim upward. At higher frame rate, an upward facing larva is observed to go immediately into a C-start [39] as it propels itself upward at *lights-off*, while the downward facing larva first tumbles before swimming upward (Video 4). An example of an upward facing larva displaying orienting behavior is shown in Video 5. We also captured a number of 25-hpf larvae that were actively swimming at the time of *lights-off*. As with stationary larvae, nearly all of the downward swimming larvae reoriented (91.6% (n=12), while only 38.9% (n=18) of upward swimming reoriented (Video 6 and Figure 3B). Interestingly, the transition from spontaneous swim to *lights-off* induced swim at 25-hpf was accompanied by an acceleration, Figure 3C (data from 10 upward- and 7 downward-swimming larvae). For both conditions (upward and downward swimming) a significant acceleration was observed following *lights-off* for the 25-hpf larvae ($p = 2.54 \times 10^{-4}$ and 2.78×10^{-2} for upward and downward, respectively).

The gravitaxis circuit is inhibitory.

As described in the introduction, the output from the antRNs to the MG appears to be inhibitory, leading us to hypothesize that the gravitaxis apparatus may operate to modulate swim responses, such as those evoked by light dimming, rather than to initiate swims. In a test of this hypothesis, we assessed whether rapidly reorienting 25-hpf larva from head-up to head-down (and vice versa) under constant light conditions would initiate swimming behavior. For this assay, larvae were embedded in 0.5% ultra-low gelling temperature agarose in sea water and then recorded horizontally (Figure 4A). Video 7 shows a representative recording. The larvae-containing petri dish was held in position for 5 minutes under constant light conditions to allow the larvae to adapt. The behavior of the larvae was then recorded for 20 seconds. While continuing to capture the behavior, the petri dish was then rotated 180 degrees (the rotation lasting ~2 seconds). The visible light was held constant for an additional 30 seconds after the rotation, at which point it was turned off and the response to *lights-off* recorded as well. As is evident in Video 7, despite being embedded in agarose the beating of the tails as the larvae attempt to swim is easily observed. To assess swim attempts we divided the duration of bouts into two categories: short swims (lasting less

than 10 frames, or ~ 1s) and long swims (>10 frames). Swim behavior was assessed from three movies, and ten upward-facing and ten downward-facing larvae were scored from each movie in three 10-second intervals: immediately before rotation, immediately after rotation, and immediately after *lights-out* (Figure 4B). The top row in Figure 4B shows head-up larvae. The first group ("10 s before rotation") showed a roughly equal distribution of behaviors, with approximately one-third showing short swims, long swims, and no swim. The second group in this row, "10 s after rotation" had been flipped from head-down to head-up by the rotation. We found no difference between these two groups ($p = 0.27$), indicating that being rotated to up-facing alone is not sufficient to evoke swimming. As a positive control for larval viability, and for our ability to detect swimming behavior, we observed that 96.7% of larvae responded to *lights-off* with long swims. Similarly, we observed no increase in swimming in larvae that were rotated to the head-down position (bottom row, Figure 4B). In fact, there was a decrease in swimming behavior of larvae that were rotated to the head-down position versus those that had been held head down for 5 minutes, seen primarily as a decrease in short swims ($p=0.04$). In summary, the results show that moving the body axis with respect to gravity does not evoke swimming, unlike *lights-off*. These results are consistent with the connectome circuity and neurotransmitter expression data indicating the output of the gravity apparatus is inhibitory.

To further investigate the nature of the gravitaxis circuit, we used the GABA receptor antagonist picrotoxin. Picrotoxin was previously used by us to demonstrate that the Group II photoreceptors - those primarily responsive to changes in ambient light, like *lights-off* - are inhibitory, while the Group I photoreceptors work via an excitatory pathway [37]. Our ability to use picrotoxin to investigate *Ciona* behavior is possible due to the paucity of GABAergic neuron types in the larval *Ciona* CNS. In addition to the Group II photoreceptors, other GABAergic cells include the eight *photoreceptor-ascending MG neuron relay neurons* (pr-AMG RNs), which are the postsynaptic targets of the Group II photoreceptors, as well as several relay interneurons that are postsynaptic of peripheral sensory nerves, and finally the antRNs [21,37,40]. As we observed previously [37], treatment of 25-hpf larvae with 1 mM picrotoxin greatly dampens the response to lights-off, but does not eliminate it (Video 8). The residual response to *lights-off* is likely due to incomplete inhibition, although there could be a contribution from the PR-Is, as described previously [37]. We focused our analysis only on picrotoxin-treated larvae showing sustained swims (> 1 second) in response to lights-off, and compared their swimming trajectories to vehicle (DMSO)-treated controls. We observed that while nearly all control larvae swam upward (96%), the picrotoxin-treated larvae showed a more equal distribution of trajectories (*i.e.*, up, down, sideways). This can be seen both in Video 8, and in five-second projection images of *lights-off* induced swims presented in Figure 4C. Behaviors were quantified in seven videos from control and picrotoxin-treated samples using two clutches of larvae, and presented as percentages (Figure 4D). In the quantification, twenty picrotoxin-treated larvae showing sustained swims were assessed from each video, as well as an equal number of controls. The distribution of swim trajectories between the two groups were significantly different ($p=1.5 \times 10^{-28}$; Wilcoxon Signed Rank Test). Picrotoxin was equally effective at disrupting gravitaxis at 21-hpf, with 61% of control (DMSO treated) larvae with sustained swims swimming upward at *lights-off*, while only 15% of picrotoxin

larvae did (p=0.00074; n= 23 and 34, respectively; Wilcoxon Signed Rank Test). In summary, these results are consistent with the inversion experiments above, and support our model that the output from the gravitaxis circuit is inhibitory.

Glutamatergic responses at 21 and 25 hpf.

We previously reported that the expression of the glutamatergic marker *vesicular glutamate transporter* (VGLUT) is restricted to sensory cells: the Group I photoreceptors, a subset of the Group II photoreceptors, the peripheral sensory neurons, and the antenna cells. As with GABAergic neurons, the limited number of VGLUT-positive neuron types in *Ciona* aids in analysis of larvae treated with pharmacological agents. Previously, we found that 25-hpf larvae treated with the AMPA receptor antagonist perampanel have disrupted phototaxis, which is mediated by glutamatergic Group I photoreceptors, but not the ability of the larvae to respond to dimming light, which is mediated by GABAergic Group II photoreceptors [37,38]. Given these observations, we predicted that larvae treated with perampanel should lose their bias for upward swimming due to inhibition of antenna cell output, while still responding to *lights-off*. At 21 hpf this is precisely the result we observed (Video 9; Figure 5A and B), with the perampanel-treated larvae no longer showing a bias for upward swimming when compared to vehicle-treated larvae ($p= 4.5 \times 10^{-13}$). Surprisingly, perampanel did not significantly disrupt gravitaxis at 25-hpf (perampanel-treated versus vehicle control p=0.37). As a control, we observed that the same group of 25-hpf perampanel-treated larvae found to have normal gravitaxis had disrupted phototaxis, Figure S2. In addition, inhibitors of NMDA receptors were found to be equally ineffective at reducing gravitaxis at 25-hpf (data not shown). Finally, *in situ* hybridization studies showed that in addition to VGLUT expression showing little obvious change from 21- to 25-hpf, no obvious differences were observed in the expression patterns of VGAT, *vesicular acetylcholine transporter* (VACHT) and AMPA receptors between 21- and 25-hpf (Figure S3).

The inability of glutamate receptor antagonists to block gravitaxis at 25-hpf might be seen as evidence that gravitaxis at this stage is mediated by something other than the antenna cell circuit. Connectomic data is only available at 21-hpf, so it is possible that new circuits have been established by 25-hpf. However, we observed that the gravitaxis response was significantly reduced at 21- and 25-hpf in the albino mutant *pristine* (Figure 5 C), which does not melanize the otolith and ocellus [38]. Previous reports have shown that melanization is essential for the function of the otolith [23,34]. Thus, the otolith is still an active component of gravitaxis at 25-hpf, and the gravitaxis response has not likely been superseded by a different system, such as the otolith-independent gravitaxis mechanism proposed in *Xenopus* larvae [16]. Moreover, the antenna cell projections from the otolith to the Ant RNs are present at 25-hpf (Figure 1A). We feel that the most likely explanation for the lack of effect on gravitaxis by glutamate receptor antagonists at 25-hpf is that the antenna cell to Ant RN synapses have transitioned to being predominantly electrical. The 21-hpf connectome shows an abundance of putative gap junctions between the antenna cells and Ant RNs, much more than was observed between the photoreceptors and their relay neurons [Figure S1, [21]], and mixed electrical/glutamatergic synapses appear to be common [41]. However, we found that continuous exposure to perampanel from 21- to 25-

hpf, did not reduce the gravitaxis response at 25-hpf, indicating that if there is a transition from chemical to electrical synapse, one does not depend on the other (data not shown). Finally, we observed a significant decrease in the response time to *lights-off* between 21- and 25-hpf larvae (Figure 5D). The number of frames from *lights-off* to the first detectable flexure of the tail was assessed (images recorded at 36 msec/frame). At 21-hpf the response time averaged 238 ± 58 ms, while at 25-hpf the response time was 188 ± 42 ms ($p = 0.015$, T-test; n= 15 larvae for each stage). Thus, there appears to be significant maturation or modulation to the gravitaxis circuit between 21- and 25-hpf. Because in assaying the reaction time we are observing the response of the circuit as a whole (including the activation of the muscles), these changes could be happening at multiple points.

A circuit model for gravitaxis.

Our time lapse videos show that *Ciona* gravitaxis behavior initiates with curved or tumbling swims triggered by *lights-off* (Figure 3A and B; Videos 3 and 4). Once the tumbling larva maneuvers to being head-up it then proceeds to swim directly upward. Straight swims are the product of symmetric and alternating activation of the left and right tail muscles, while curved or tumbling swims are the product of asymmetric left or right activation or inhibition. Based on our observations that curved or tumbling behavior ceases when the larvae is head-up, and that more than half of larvae facing or swimming upward go directly into symmetric swims at *lights-off*, a simple model would be that the gravitaxis circuit evokes asysmmetric swimming when the larva is head-down or sideways, but this circuit is off (or at least less active) when the larva is facing upward. In addition, the *Ciona* connectome shows that the projections from Ant RNs go predominantly to the right MGINs and MNs [21]. Our VGAT expression [37] and behavior studies (Figure 4) indicate that these asymmetric Ant RN projections are inhibitory. We incorporate these two components (*i.e.*, gravitaxis response is on when head is down and off when head is up, and asymmetric inhibition from the Ant RNs) into a circuit model of gravitaxis (Figure 6). The inhibitory nature of the gravitaxis output would account for the observation that the majority of larvae before *lights-off* are head down and stationary (*i.e.*, the gravitaxis circuit alone does not evoke swimming). However, we also observed a number of larvae swimming directly downward before *lights-off*, and then immediate changing course and begin swimming upward (e.g., Figure 3B, and Video 6), and overall, spontaneous swims before *lights-off* showed little or no upward bias (Figure 2C). Therefore, the gravitaxis circuit appears to be either turned on by *lights-off*, or actively repressed until *lights-off*. The circuity and neurotransmitter use data support the second option. The *lights-off* response is mediated by the Group II photoreceptors [37,38], and the connectome shows that there are only two places where there is extensive intersection of the gravitaxis and Group II photoreceptor circuits [21]. One is at the cholinergic MGINs in the MG, and the other is in the posterior BV at the level of the relay neurons (Figure 6). Connectomic, VGAT expression, behavior, and pharmacology data are all consistent with the Group II photoreceptors being inhibitory. The primary postsynaptic targets of the Group II photoreceptors are the GABAergic pr-AMG RNs, located in the posterior BV. The pr-AMG RNs then project to the cholinergic MGINs in the MG (Figure 6). These observations, as well as pharmacological studies, lead to the hypothesis that the Group II photoreceptors activate swimming by inhibiting the pr-AMG RNs, which in turn releases inhibition of the MGINs (*i.e.*, a disinhibition) [37]. Significantly, the pr-AMG RNs

also make extensive chemical synaptic contacts with the Ant RNs in the posterior BV, where they could potentially antagonize this circuit (Figures 6 and S4). These inhibitory synaptic contacts make a plausible circuit model that would account for the behavioral observations. For example, in a stationary downward facing larva (Figure 6A), the antenna cells would be signaling but the Ant RNs would be inhibited by the pr-AMG RNs. Shutting the light off would release the inhibition both on the MGINs, initiating swimming, and on the Ant RNs, leading to asymmetric inhibition on the MGIN and MNs. Importantly, the inhibition of the Ant RNs by the pr-AMG RNs can explain the ability of larvae to spontaneously swim downward, yet immediately go into a turn at *lights-off* (Figure 6B). The other primary intersection of these two circuits, at the MGINs, does not readily suggest a circuit logic that can account for this behavior. This same circuit can also account for the behavior of upward facing larvae. In this case the antenna cells are less active (or off), and thus *lights-off* can lead to immediate symmetric swimming (Figure 6C). Further evidence from this model comes from our observation that spontaneously swimming larvae accelerate at *lights-off* (Figure 3C). The model predicts that the inhbitory pr-AMG RNs are active during the spontaneous swim (Figure 6D), and thus *lights-off* could release this inhibition on the MGINs, accounting for the acceleration.

DISCUSSION

In most tunicate species the larva is a transient entity. In ascidians (the Class of tunicates to which *Ciona* belongs) the larva persist for only a day or two before attaching via its adhesive palps to a solid substrate. Once attached, larva undergoes metamorphosis, resulting in a sessile adult body form which has little resemblance to the tadpole-like larva [42]. Larval behavior is thought to change over the course of the day to serve different needs: first to disperse from the locale where they were spawned, and then to find a suitable settling place [15,24,43]. Upward swimming may aid in attachment of ascidians, which are often found on the underside of docks and other structures. This raises questions concerning the behaviors described here: what function do they serve, and are the differences observed at 21-hpf and 25-hpf part of a program of adaptive behaviors, or simply a reflection of the maturation of the underlying circuitry? Both 21- and 25-hpf larvae respond equally well to lights-off (*i.e.*, greater than 90% responding at both stages), implying that the visual system is fully developed by 21-hpf. However, the 21-hpf swims have lower velocity, are more tortuous, and have a less of an upward bias. We speculated that dimming-induced swims may be a manifestation of the looming shadow defense response found widely in animals [44]. Similar dimming-induced upward swimming behavior has been observed in vertebrate larvae, specifically *Xenopus* and cave fish *Astyanax mexicanus* [17,45], suggesting that light dimming-induced upward swimming behavior may be a conserved chordate behavior. In fact, the *Xenopus* behavior is thought to aid in the attachment of the young larva to the underside of rocks or vegetation via the adhesive cement gland. In addition, the response in both *Xenopus* and *Astyanax* is mediated by the pineal eye, and we have speculated that the *Ciona* Group II photoreceptor complex may be homologous to the vertebrate pineal eye, while the Group I may be homologous to the lateral eye [37]. In summary, the 21-hpf behavior would appear to be better suited as an escape behavior (*i.e.*, more tortuous and with a less predictable direction), while the 25-hpf behavior may be more appropriate for

attachment, suggesting that these may be distinct behaviors. The mechanism responsible for the behavioral transitions observed between 21- and 25-hpf is not known. The *Ciona* connectome is from a 21-hpf larva so synaptic modifications between these two stages remain to be determined, but the persistence of the gravitaxis behavior in the presence of glutamate receptor inhibitors (unlike at 21-hpf) suggests possible mechanisms, as does the change in reaction time.

We present a circuit model (Figure 6) that can account for the observed behavior of *Ciona* larvae, and that is consistent with neurotransmitter use and connectomic data [21,37]. Because the connectome is from a 21-hpf larva, we can have the most confidence in the model for this stage. Our data indicate that the gravitaxis circuit is not acting to initiate swimming behavior, but rather to modulate swims through asymmetric inhibition, resulting in curved or tumbling swims. Moreover, our observation that the gravitaxis circuit is more active in downward facing than upward facing larvae suggests a simple mechanism for larvae to orient themselves with respect to gravity. Key components in our model are the pr-AMG RNs. We hypothesize that their inhibition of the Ant RNs before *lights-off* can account for the ability of larvae to swim down or sideways, but then to quickly reorient to swim upward at *lights-off*. While we have previously presented evidence that the pr-AMG RNs are inhibitory [37], our model requires that these neurons be constitutively active until inhibited by the Group II photoreceptors at *lights-off*. Our evidence for this is limited to the observations that larvae of the mutant *frimousse*, which have disrupted relay neuron input to the MG, as well as larvae in the presence of GABA receptor inhibitors, which have elevated spontaneous swimming, implying a tonic inhibition of swimming in normal larvae [37]. However, direct observation of these circuits will be required to confirm the model.

STAR METHODS

CONTACT FOR DATA AND REAGENTS

Requests for further information regarding data or reagents used in this study should be directed to the lead author, William C. Smith (w_smith@ucsb.edu).

EXPERIMENTAL MODEL AND SUBJECT DETAILS

Adult *Ciona robusta* [also known *Ciona intestinalis* type A [46]] were collected at the Santa Barbara Harbor, with the exception of the mutant *pristine*, which was cultured at the UC Santa Barbara Marine Laboratory, a continuous-flow seawater system [47]. Gametes were dissected from adults and crossed *in vitro* to generate larvae, or in the case of *pristine*, adults were spawned using a light/dark cycle [47]. All embryos and larvae were cultured at 18°C.

METHODS DETAILS

Drug Treatments—Peramapanel (Adooq) was dissolved in DMSO at 4.3 mM and then diluted in seawater to final concentration of 20 μm. Control larvae received DMSO only at 0.47%. Picrotoxin (Tocris) was dissolved in DMSO to make a 40 mM stock solution, and then added to a final concentration of 1 mM. Control larvae received DMSO at 2.5%. Larvae were incubate with perampanel or picrotoxin a minimum of 10 minutes before assaying. To visualize antenna cells, *Ciona intestinalis* type B eggs (Marine Biological Laboratory, Woods

Hole), were microinjected [47] with a VGLUT-kaede expression plasmid [48]. Chain reaction *in situ* hybridization (HCR) was performed according to the manufacturer's protocol (Molecular Instruments) and imaged using Imaris software.

Gravitaxis Assays—For imaging gravitaxis behavior, 500 larvae of the appropriate stage were added to a 6 cm petri dishes containing filtered seawater plus 0.1% BSA. For pharmacological studies the BSA was omitted and instead the inside of the petri dish was coated with a 1% agarose solution to discourage sticking. The petri dishes were then covered with an inverted lid while trapping no air bubbles, and the edges sealed with high vacuum grease (Dow Corning) to allow the dish to be held vertically without leaking. The petri dish was then mounted in the flanged end of a 2 inch PVC pipe held horizontally with a clamp that would allow for rotation. Time-lapse images were collected with a horizontally mounted Hamamatsu ORCA-ER camera fitted with a Navitar Zoom 7000 lens and red filter (Tiffen). Images were recorded using a 700 nm LED lamp, while visible light was modulated with a 505 nm LED lamp (both from Mightex). Except for when stated otherwise the LED lamps were mounted above the petri dishes. Most behaviors were captured at 8.9 frames/second. Certain behaviors were captured at 27.9 frames/second, and these imaging sessions are referred to as "high speed" in the Results.

QUANTIFICATION AND STATISTICAL ANALYSIS

Spontaneous and induced swim directions were assayed from three different clutches of larvae at each developmental stage, and three or more recordings were made from each clutch of larvae with a five-minute recovery period between assays. Swim direction was assessed from 20 randomly selected larvae from each recording, and the net movement over 5 seconds (up, down, or sideways, see Figure 2C) from the starting to ending positions were manually assigned with the aid of the Fiji software package [49]. In the assessments, larvae laying on the bottom surface were not counted, nor where those stuck to the petri dish or that collided with the side of the petri dish or other larvae. Only swims persisting for at least 10 frames (~1 second) were scored (*i.e.*, short tail flicks were not scored as swims). The percentages in the three directional categories were calculated for each recording. The averages of these, as well as the standard deviation between recordings, is shown in Figure 2C. To compare gravitaxis behavior between conditions (Figure 2D), directional scores of all larvae from each condition were compiled and assigned a value (down=1, sideways = 2, up = 3). The compiled scores between conditions were then tested for significance using the Wilcoxon Signed Rank Test. Swim velocity and tortuosities were calculated using a Matlab script (available upon request) [37]. Finally, percentages of larvae swimming was calculated by scoring all larvae within a central 400×400 pixel square of a 5-second time-lapse recording as either swimming for >10 frames or not. The number of larvae scored in the designated 400×400 pixel squares varied from 23–57.

Supplementary Material

Refer to Web version on PubMed Central for supplementary material.

ACKNOWLEDGMENTS.

We thank Yasunori Sasakura and the Japanese National Bioresource Project for the gift of plasmids, and Kerrianne Ryan for her helpful comments on the manuscript. This work was supported by an award from NIH (NS103774) to W.C.S.

References

1. Häder D-P, and Hemmersbach R. (2017). Gravitaxis in Euglena In Euglena:Biochemistry, Cell and Molecular Biology Advances in Experimental Medicine and Biology, Schwartzbach SD and Shigeoka S, eds. (Cham: Springer International Publishing), pp. 237–266. Available at: 10.1007/978-3-319-54910-1_12 [Accessed September 27, 2019].
2. Laurens J, Meng H, and Angelaki DE (2013). Neural Representation of Orientation Relative to Gravity in the Macaque Cerebellum. Neuron 80, 1508–1518. [PubMed: 24360549]
3. Nakamura M, Nishimura T, and Morita MT (2019). Gravity sensing and signal conversion in plant gravitropism. J. Exp. Bot 70, 3495–3506. [PubMed: 30976802]
4. Beraneck M, Lambert FM, and Sadeghi SG (2014). Chapter 15 - Functional Development of the Vestibular System: Sensorimotor Pathways for Stabilization of Gaze and Posture In Development of Auditory and Vestibular Systems, Romand R. and Varela-Nieto I, eds. (San Diego: Academic Press), pp. 449–487. Available at: http://www.sciencedirect.com/science/article/pii/B9780124080881000154 [Accessed September 27, 2019].
5. Favre-Bulle IA, Stilgoe AB, Rubinsztein-Dunlop H, and Scott EK (2017). Optical trapping of otoliths drives vestibular behaviours in larval zebrafish. Nat. Commun 8, 1–7. [PubMed: 28232747]
6. Hama N, Tsuchida Y, and Takahata M. (2007). Behavioral context-dependent modulation of descending statocyst pathways during free walking, as revealed by optical telemetry in crayfish. J. Exp. Biol 210, 2199–2211. [PubMed: 17562894]
7. Levi R, Varona P, Arshavsky YI, Rabinovich MI, and Selverston AI (2004). Dual Sensory-Motor Function for a Molluskan Statocyst Network. J. Neurophysiol 91, 336–345. [PubMed: 14507988]
8. Tamm SL (2015). Functional Consequences of the Asymmetric Architecture of the Ctenophore Statocyst. Biol. Bull 229, 173–184. [PubMed: 26504158]
9. Aoyagi M, Kimura M, and Yagi T. (2003). The effect of gravity on the stability of human eye orientation. Auris. Nasus. Larynx 30, 363–367. [PubMed: 14656561]
10. Peterka RJ (2018). Sensory integration for human balance control. Handb. Clin. Neurol 159, 27–42. [PubMed: 30482320]
11. Bagnall MW, and Schoppik D. (2018). Development of vestibular behaviors in zebrafish. Curr. Opin. Neurobiol 53, 83–89. [PubMed: 29957408]
12. De Meester L. (1991). An analysis of the phototactic behaviour of Daphnia magna clones and their sexual descendants. Hydrobiologia 225, 217–227.
13. Gravinese PM (2018). Vertical swimming behavior in larvae of the Florida stone crab, Menippe mercenaria. J. Plankton Res 40, 643–654.
14. Janse C. (1982). GRAVITY ORIENTATION IN GASTROPOD MOLLUSCS In Exogenous and Endogenous Influences on Metabolic and Neural Control, Addink ADF and Spronk N, eds. (Pergamon), p. 220 Available at: http://www.sciencedirect.com/science/article/pii/B978008028845150130X [Accessed October 1, 2019].
15. Svane IB, and Young CM (1989). The ecology and behavior of ascidian larvae. Mar Biol Rev 27.
16. Roberts A, Hill NA, and Hicks R. (2000). Simple mechanisms organise orientation of escape swimming in embryos and hatchling tadpoles of Xenopus laevis. J. Exp. Biol 203, 1869–1885. [PubMed: 10821744]
17. Yoshizawa M, and Jeffery WR (2008). Shadow response in the blind cavefish Astyanax reveals conservation of a functional pineal eye. J Exp Biol 211, 292–9. [PubMed: 18203983]
18. Okumura E, Tanaka R, and Yoshiga T. (2013). Negative gravitactic behavior of Caenorhabditis japonica dauer larvae. J. Exp. Biol 216, 1470–1474. [PubMed: 23307800]

19. Sun Y, Liu L, Ben-Shahar Y, Jacobs JS, Eberl DF, and Welsh MJ (2009). TRPA channels distinguish gravity sensing from hearing in Johnston's organ. Proc. Natl. Acad. Sci 106, 13606–13611. [PubMed: 19666538]
20. White JG, Southgate E, Thomson JN, and Brenner S. (1986). The structure of the nervous system of the nematode Caenorhabditis elegans. Philos Trans R Soc Lond B Biol Sci 314, 1–340. [PubMed: 22462104]
21. Ryan K, Lu Z, and Meinertzhagen IA (2016). The CNS connectome of a tadpole larva of Ciona intestinalis (L.) highlights sidedness in the brain of a chordate sibling. Elife 5.
22. Chen W-L, Ko H, Chuang H-S, Bau HH, and Raizen D. (2019). Caenorhabditis elegans Exhibits Positive Gravitaxis. bioRxiv, 658229.
23. Jiang D, Tresser JW, Horie T, Tsuda M, and Smith WC (2005). Pigmentation in the sensory organs of the ascidian larva is essential for normal behavior. J Exp Biol 208, 433–8. [PubMed: 15671331]
24. Kajiwara S, and Yoshida M. (1985). Changes in Behavior and Ocellar Structure during the Larval Life of Solitary Ascidians. Biol. Bull 169, 565–577.
25. Tsuda M, Sakurai D, and Goda M. (2003). Direct evidence for the role of pigment cells in the brain of ascidian larvae by laser ablation. J Exp Biol 206, 1409–17. [PubMed: 12624175]
26. Berrill NJ THE DEVELOPMENT AND GROWTH OF CIONA. Journal of the Marine Biological Association of the United Kingdom 26, 616–625.
27. Bone Q. (1992). On the locomotion of ascidian tadpole larvae. J Mar Biol Assoc U K 72, 161–186.
28. Zega G, Thorndyke MC, and Brown ER (2006). Development of swimming behaviour in the larva of the ascidian Ciona intestinalis. J Exp Biol 209, 3405–12. [PubMed: 16916975]
29. Delsuc F, Brinkmann H, Chourrout D, and Philippe H. (2006). Tunicates and not cephalochordates are the closest living relatives of vertebrates. Nature 439, 965–8. [PubMed: 16495997]
30. Hudson C. (2016). The central nervous system of ascidian larvae. Wiley Interdiscip Rev Dev Biol.
31. Horie T, Kusakabe T, and Tsuda M. (2008). Glutamatergic networks in the Ciona intestinalis larva. J Comp Neurol 508, 249–63. [PubMed: 18314906]
32. Imai JH, and Meinertzhagen IA (2007). Neurons of the ascidian larval nervous system in Ciona intestinalis: I. Central nervous system. J Comp Neurol 501, 316–34. [PubMed: 17245701]
33. Eakin RM, and Kuda A. (1971). Ultrastructure of sensory receptors in Ascidian tadpoles. Z Zellforsch Mikrosk Anat 112, 287–312. [PubMed: 5542324]
34. Sakurai D, Goda M, Kohmura Y, Horie T, Iwamoto H, Ohtsuki H, and Tsuda M. (2004). The role of pigment cells in the brain of ascidian larva. J Comp Neurol 475, 70–82. [PubMed: 15176085]
35. Hughes I, Thalmann I, Thalmann R, and Ornitz DM (2006). Mixing model systems: Using zebrafish and mouse inner ear mutants and other organ systems to unravel the mystery of otoconial development. Brain Res. 1091, 58–74. [PubMed: 16529728]
36. Léger S, and Brand M. (2002). Fgf8 and Fgf3 are required for zebrafish ear placode induction, maintenance and inner ear patterning. Mech. Dev 119, 91–108. [PubMed: 12385757]
37. Kourakis MJ, Borba C, Zhang A, Newman-Smith E, Salas P, Manjunath B, and Smith WC (2019). Parallel visual circuitry in a basal chordate. eLife 8.
38. Salas P, Vinaithirthan V, Newman-Smith E, Kourakis MJ, and Smith WC (2018). Photoreceptor specialization and the visuomotor repertoire of the primitive chordate Ciona. J Exp Biol 221.
39. Müller UK, and Leeuwen J.L. van (2004). Swimming of larval zebrafish: ontogeny of body waves and implications for locomotory development. J. Exp. Biol 207, 853–868. [PubMed: 14747416]
40. Ryan K, Lu Z, and Meinertzhagen IA (2018). The peripheral nervous system of the ascidian tadpole larva: Types of neurons and their synaptic networks. J Comp Neurol 526, 583–608. [PubMed: 29124768]
41. Serrano-Velez JL, Rodriguez-Alvarado M, Torres-Vazquez II, Fraser SE, Yasumura T, Vanderpool KG, Rash JE, and Rosa-Molinar E. (2014). Abundance of gap junctions at glutamatergic mixed synapses in adult Mosquitofish spinal cord neurons. Front. Neural Circuits 8 Available at: https://www.ncbi.nlm.nih.gov/pmc/articles/PMC4072101/ [Accessed October 10, 2019].
42. Chiba S, Sasaki A, Nakayama A, Takamura K, and Satoh N. (2004). Development of Ciona intestinalis Juveniles (Through 2nd Ascidian Stage). Zoolog. Sci 21, 285–298. [PubMed: 15056923]

43. Millar RH (1971). The Biology of Ascidians In Advances in Marine Biology, Russell FS and Yonge M, eds. (Academic Press), pp. 1–100. Available at: http://www.sciencedirect.com/science/article/pii/S0065288108603417 [Accessed October 20, 2019].

44. Peek MY, and Card GM (2016). Comparative approaches to escape. Curr Opin Neurobiol 41, 167–173. [PubMed: 27710794]

45. Jamieson D, and Roberts A. (2000). Responses of young Xenopus laevis tadpoles to light dimming: possible roles for the pineal eye. J Exp Biol 203, 1857–67. [PubMed: 10821743]

46. Brunetti R, Gissi C, Pennati R, Caicci F, Gasparini F, and Manni L. (2015). Morphological evidence that the molecularly determined Ciona intestinalis type A and type B are different species: Ciona robusta and Ciona intestinalis. J. Zool. Syst. Evol. Res 53, 186–193.

47. Veeman MT, Chiba S, and Smith WC (2011). Ciona genetics. Methods Mol Biol 770, 401–22. [PubMed: 21805273]

48. Horie T, Shinki R, Ogura Y, Kusakabe TG, Satoh N, and Sasakura Y. (2011). Ependymal cells of chordate larvae are stem-like cells that form the adult nervous system. Nature 469, 525–8. [PubMed: 21196932]

49. Schindelin J, Arganda-Carreras I, Frise E, Kaynig V, Longair M, Pietzsch T, Preibisch S, Rueden C, Saalfeld S, Schmid B, et al. (2012). Fiji: an open-source platform for biological-image analysis. Nat. Methods 9, 676–682. [PubMed: 22743772]

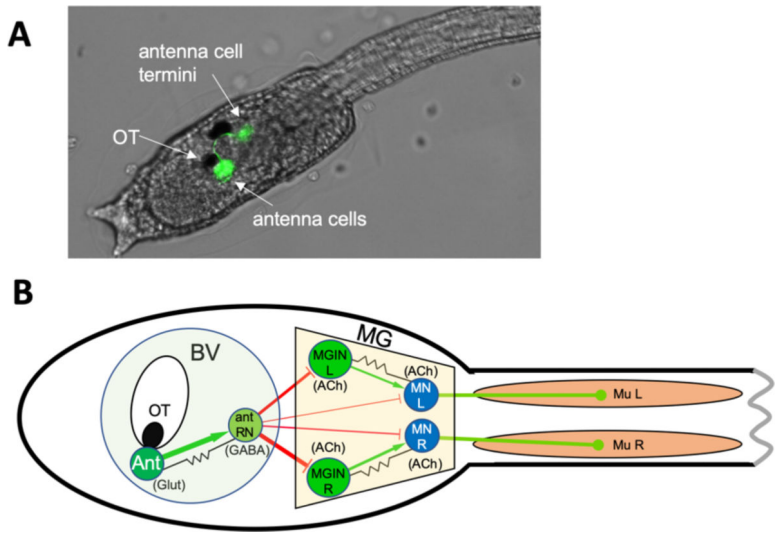

Figure 1. Ciona gravitaxis circuit.

A. Twenty-five hours post-fertilization (hpf) larva expressing Kaede fluorescent protein from an injected plasmid containing the vesicular glutamate transporter (VGLUT) cis-regulatory element. The antenna cells are green. **B.** Simplified minimal gravitaxis circuit. Cells of similar type and connectivity (circles) and their synaptic connections (lines) were combined based on connectome data from a 21-hpf larva. Cell types includes the two antenna cells (Ant), the eleven antenna relay neurons (Ant RN), the three left and right motoganglion interneurons (MGIN L and MGIN R, respectively), the five left and right motor neurons (MN L and MN R, respectively), and the 18 left and right muscles (Mu L and Mu R, respectively). Likely neurotransmitter types derived from in situ hybridization studies are indicated (Glut: glutamate; GABA: gamma-aminobutyric acid; ACh: acetylcholine), as well as putative excitatory (green), inhibitory (red) and electrical (gap junction) synapses (black). Other abbreviations: OT: otolith cell, BV: brain vesicle; MG: motor ganglion.

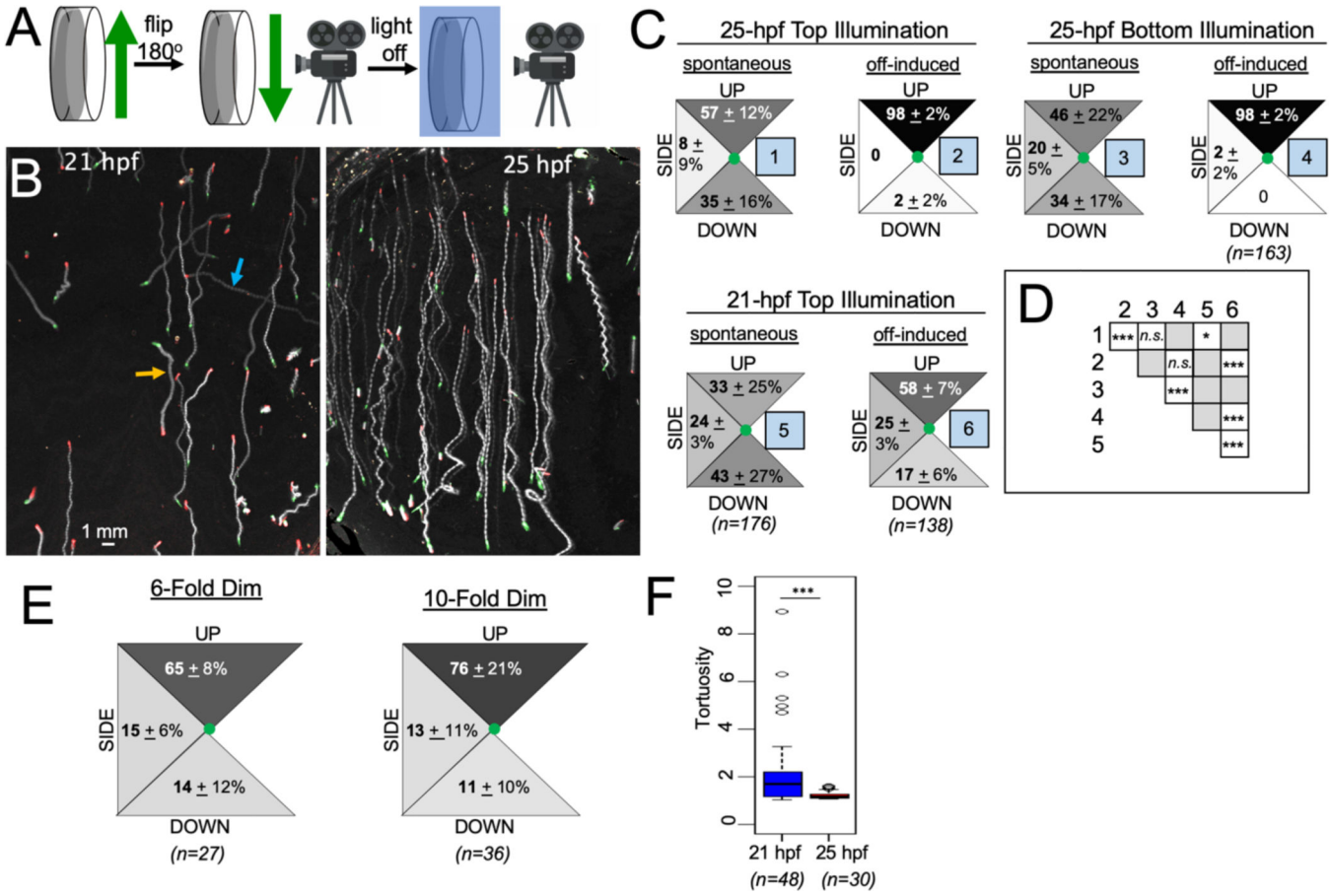

Figure 2. Ciona gravitaxis behavior.

A. Imaging set-up for recording gravitaxis behavior. **B**. Five-second projection images of 21- and 25-hour post fertilization (hpf) larvae swimming in response to the turning off of visible light (lights-off condition; swim traces in white on dark background). The beginning position of larvae is indicated in green and their position after 5 seconds is in red. Up is towards the top of the images. The orange arrow indicates a larva swimming downward and the blue arrow indicates a larva swimming sideways. **C.** Quantified swim trajectory data for swims under the indicated conditions and developmental ages. Percentages of larvae within the categorized trajectories [(UP, DOWN and SIDE (sideways)] are shown. Values are from the averages of nine videos (± standard deviation), with 20 larvae assessed per video. **D.** Matrix comparing the compiled swim data from different conditions (numbered as in **C**) for significant differences. (*: $p < 0.05$; ***: $p<0.005$; Wilcoxon Signed Rank Test). **E**. Quantified swim trajectory data for 25-hpf larvae in response to 6- and 10-fold dimming of visible light. **F.** lights-off induced swims are more tortuous at 21-hpf than at 25-hpf (***: $p <0.005$; Wilcoxon Ranksum Test).

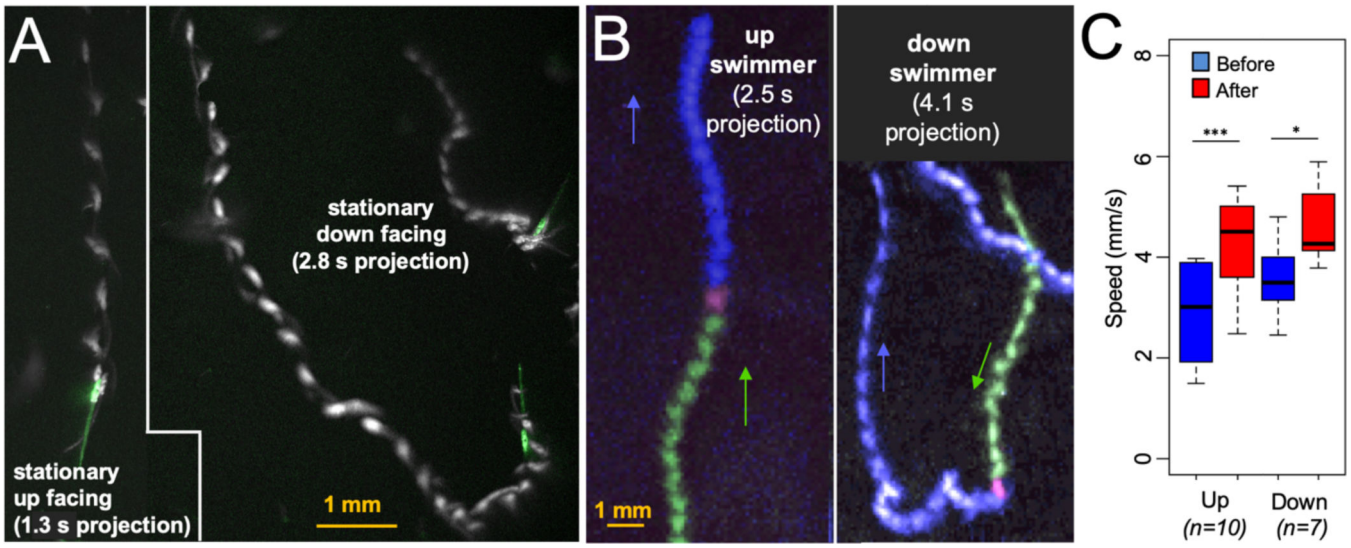

Figure 3. Reorientation Behavior.

A. Response of stationary up-facing and down-facing larvae to lights-off. The initial position of larvae are shown in green, and swims are projected over time in white. **B.** Response of swimming larvae to lights-off. Projection images of larvae show the trajectory before lights-off (green) and after (blue). Magenta marks the first frame of lights-off. **C.** Both upward and downward swimmers accelerate at lights-off. Swim speeds before and after lights-off are indicated (*: $p<0.05$; ***: $p<0.005$; T-test).

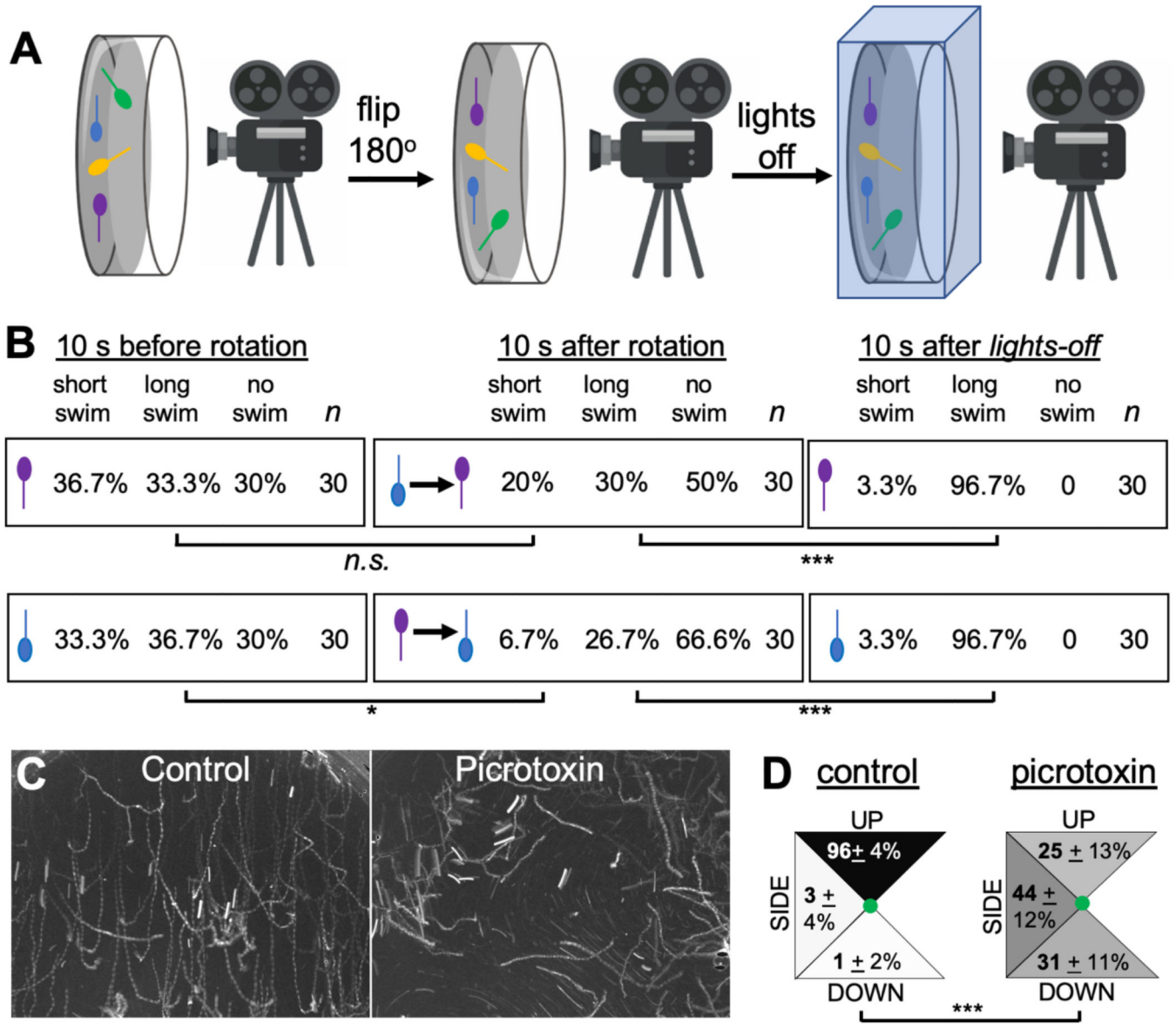

Figure 4. Gravitaxis response is inhibitory.

A. Imaging set-up used to record behavioral response of Ciona larvae to being rotated with respect to gravity. **B.** Results of rotation experiments. The top row shows up-facing larvae immediately before rotation, immediately after rotation, or after visible light is turned off. The bottom row shows the same conditions, but with down-facing larvae. The results show the percentage of larvae in 10-second windows displaying short, long, or no swims. For comparisons between groups, swim categories were assigned values and assessed with the Wilcoxon Signed Rank Test (*: $p<0.05$; *** $p<0.005$). **C.** Five-second projection images showing swims in control and picrotoxin-treated larvae. Swims appear as white lines. Up is toward the top of the image. **D.** Quantification of swim trajectories in control and picrotoxin-treated larvae, analyzed as in Figure 2C.

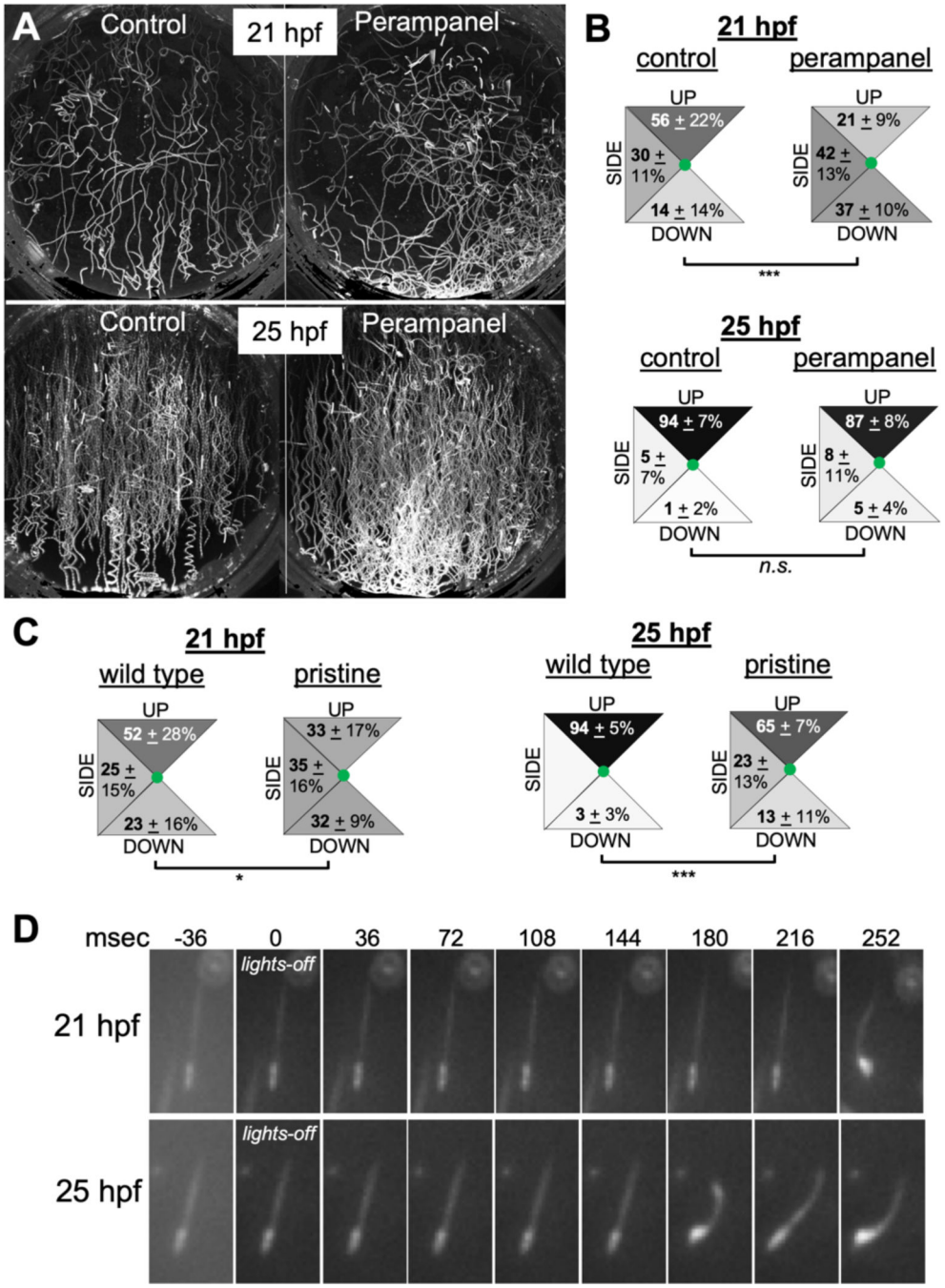

Figure 5. Gravitaxis comparisons in 21- and 25-hours post fertilization larvae.

A. Control (DMSO vehicle) and perampanel-treated larvae. Shown are 10-second projections of swims following lights-off. Larvae were assessed at 21- and 25 hours post fertilization (hpf). **B.** Quantification of swim trajectory in control and perampanel-treated larvae. Shown are the swim trajectories [UP, DOWN or SIDE (sideways)] in five second windows following lights-off. The values are averages from 10 time-lapse videos (20 larvae analyzed per video) plus or minus standard deviations. For comparisons between groups, swim directions were assigned values and assessed with the Wilcoxon Signed Rank Test. **C**.

Swim directions following lights-off in wild-type and homozygous pristine mutants. The analysis was performed as in B (*: $p<0.05$; *** $p<0.005$). **D.** Frames from time-lapse recordings showing representative reaction times to lights-off at 21- and 25-hpf. Times in milliseconds (msec) are indicated.

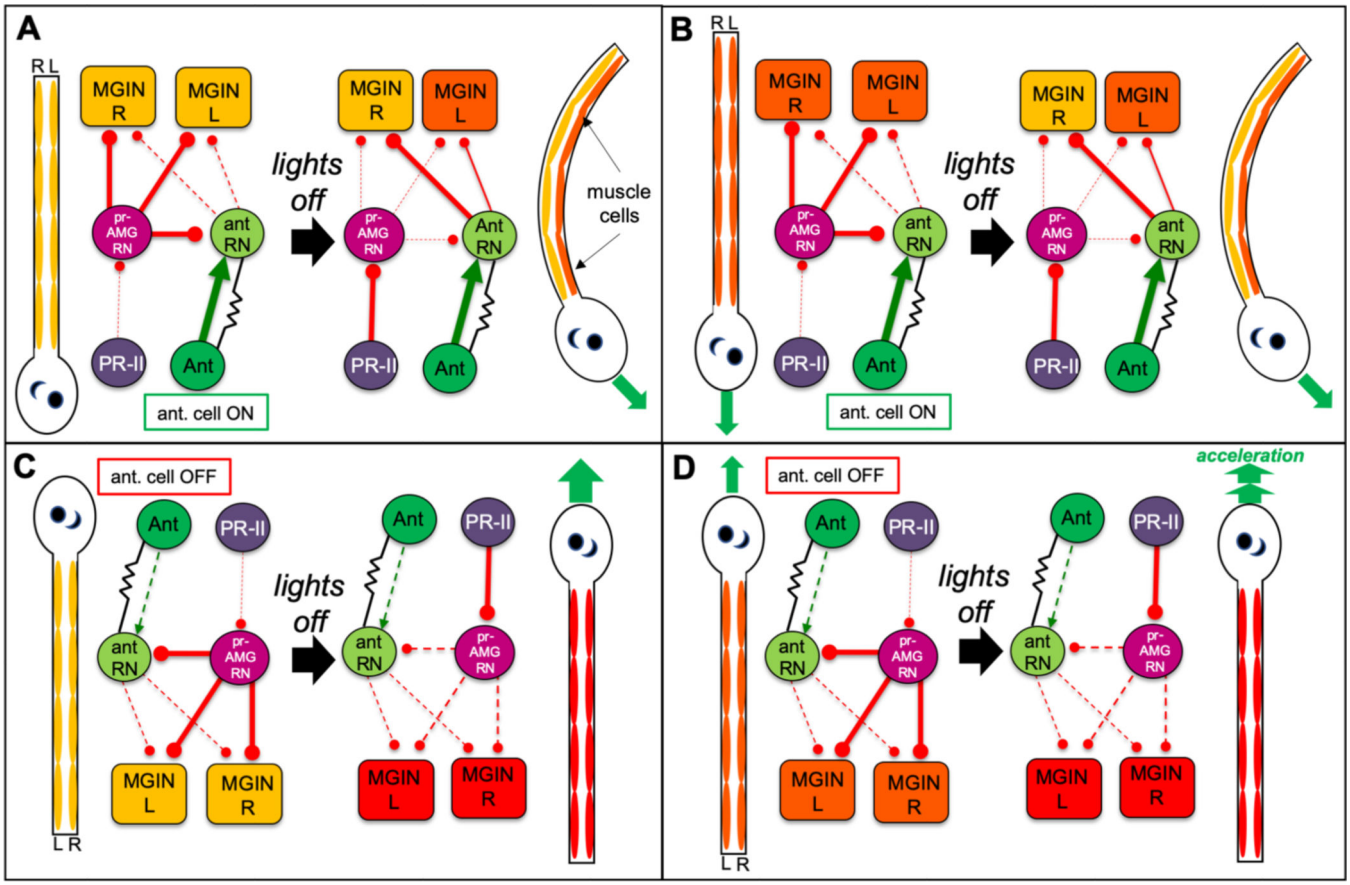

Figure 6. Model of Gravitaxis Circuitry.

Each panel shows both a cartoon larva with the relative activation of the muscle cells shown from low (yellow), to intermediate (orange) and high (red), and a diagram of the gravitaxis and photoreceptor circuits. In the circuit diagrams, proposed inhibitory synaptic projections are in red, excitatory are in green, and electrical in black. **A.** Behavior and circuitry of a down-facing larva before (left), and after (right) visible light being turned off (lights-off). Asymmetric inhibition from the antRNs leads to asymmetric L/R muscle activation and turning (green arrow). **B**. Behavior and circuitry of downward swimming larva. Note that inhibition of the antRNs by the pr-AMG RNs allows for symmetrical activation of muscles (orange) before lights-off. **C.** Behavior and circuitry of up-facing larva. Note that the antenna cells are inactive when the larva is in this position. At lights-off the larvae can go directly to symmetric swim. **D.** Behavior and circuitry of upward swimming larva. In the model release of inhibition by the pr-AMG RNs on the MGINs at lights-out leads to acceleration. Abbreviations: PR-II: photoreceptor group II; pr-AMG RN: photoreceptor-ascending motor ganglion relay neurons; Ant: antenna cells; antRN: antenna relay neurons; MGIN: motor ganglion interneurons; R: right: L: left.

KEY RESOURCE TABLE

REAGENT or RESOURCE	SOURCE	IDENTIFIER
Chemicals, Peptides, and Recombinant Proteins		
Perampanel	Adooq Bioscience	A12498
Picrotoxin	Tocris	1128
Fluorescently labeled probes for VGAT, VACHT and AMPA	Molecular Instruments	https://www.molecularinstruments.com
Experimental Models: Organisms/Strains		
Ciona robusta wild caught (formerly *Ciona intestinalis* type A)	Santa Barbara Harbor	NA
Ciona intestinalis (formerly *Ciona intestinalis* type B)	Marine Biological Laboratory, Woods Hole	NA
Recombinant DNA		
C. robusta vglut>kaede	Yasunori Sasakura, University of Tsukuba, Japan	NA
Software and Algorithms		
Fiji	NIH Image	https://imagej.net/Fiji
MATLAB	WolframAlpha	https://www.wolframalpha.com
Imaris v 9.1	Bitplane	https://imaris.oxinst.com
Other		
ORCA-ER camera	Hamamatsu	https://camera.hamamatsu.com
ZOOM 7000 with manual zoom	Navitar	ZOOM 7000
52mm red 25 filter	Tiffen	52R25
BioLED optical head, Precision LED Spot light, 700 nm	Mightex Systems	BLS-PLS-0700-01-S
BioLED optical head, Precision LED Spot light, 505 nm	Mightex Systems	BLS-PLS-0505—030–04
BioLED light source control module	MIghtex Systems	BLS-SA04-US